ELSEVIER

Contents lists available at ScienceDirect

Chemosphere

journal homepage: www.elsevier.com/locate/chemosphere





Acidic process fluid from hydrothermal carbonization improves dechlorination of waste PVC and produces clean solid and liquid fuels

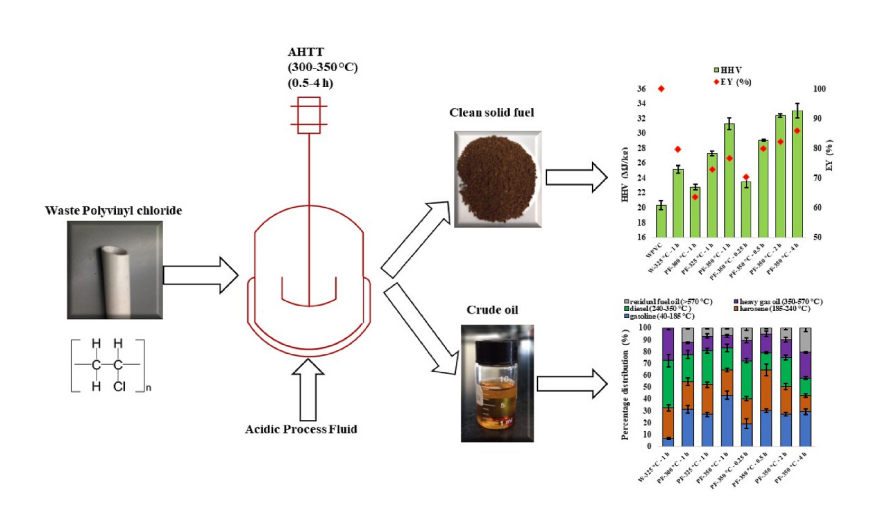
Vahab Ghalandari, Toufiq Reza

Department of Chemistry and Chemical Engineering, Florida Institute of Technology, 150 West University Boulevard, Melbourne, FL, 32901, USA

HIGHLIGHTS

- Acidic process fluid improves dechlorination of waste PVC through AHTT.
- AHTT's char has higher ignition temperature and lower burnout temperature.
- The char has low slagging, fouling and alkali indexes, and chlorine content.
- The HHV of the AHTT's crude oil are between 26.11 and 34.6 MJ/kg.

GRAPHICAL ABSTRACT



ARTICLE INFO

Handling editor. Pouria Ahmadi

Keywords:
Hydrothermal treatment
Waste plastics
HTC process fluid
Dechlorination
Solid fuel
Crude oil

ABSTRACT

Dechlorination of waste PVC (WPVC) by hydrothermal treatment (HTT) is a potential technology for upcycling WPVC in order to create non-toxic products. Literature suggests that acids can improve the HTT process, however, acid is expensive and also results in wastewater. Instead, the acidic process fluid (PF) of hydrothermal carbonization (HTC) of orange peel was utilized in this study to enhance the dechlorination of WPVC during HTT. Acidic HTT (AHTT) experiments were carried out utilizing a batch reactor at 300–350 °C, and 0.25–4 h. The finding demonstrated that the dechlorination efficiency (DE) is high, which indicates AHTT can considerably eliminate chlorine from WPVC and relocate to the aqueous phase. The maximum DE of 97.57 wt% was obtained at 350 °C and 1 h. The AHTT temperature had a considerable impact on the WPVC conversion since the solid yield decreases from 56.88 % at 300 °C to 49.85 % at 350 °C. Moreover, AHTT char and crude oil contain low chloride and considerably more C and H, leading to a considerably higher heating value (HHV). The HHV increased from 23.48 to 33.07 MJ/kg when the AHTT time was raised from 0.25 to 4 h at 350 °C, indicating that the AHTT time has a beneficial effect on the HHV. The majority fraction of crude oil evaporated in the boiling range of lighter fuels include gasoline, kerosene, and diesel (57.58–83.09 wt%). Furthermore, when the AHTT temperature was raised from 300 to 350 °C at 1 h, the HHV of crude oils increased from 26.11 to 33.84 MJ/kg.

E-mail address: treza@fit.edu (T. Reza).

^{*} Corresponding author.

Crude oils derived from AHTT primarily consisted of phenolic (50.47-75.39 wt%), ketone (20.1-36.34 wt%), and hydrocarbon (1.08-7.93 wt%) constituents. In summary, the results indicated that AHTT is a method for upcycling WPVC to clean fuel.

Nomenclature

Symbols	Definition
AHTT	Acidic hydrothermal treatment
DCM	Dichloromethane
DE	Dechlorination efficiency
EY	Energy yield
FC	Fixed carbon
HHV	Higher heat value
HTC	Hydrothermal carbonization
HTT	Hydrothermal treatment
I_A	Alkali index
I_{F}	Fouling index
I_S	Slagging index
I_V	Slag viscosity index
PF	Acidic process fluid
S	Comprehensive combustibility index
SY	Solid yield
VM	Volatile matter
WPVC	Waste polyvinyl chloride

1. Introduction

Plastics are used in many aspects of day-to-day life due to the many benefits they provide, including excellent resistance to corrosion, inexpensive production costs, durability, low weight, and excellent flexibility (M. Shen et al., 2022; Rahimi and García, 2017; Nyberg et al., 2023; Tejaswini et al., 2022). In 2021, around 390.7 million tons of plastic were produced all over the world (Abelouah et al., 2023). Polyvinyl chloride (PVC) is one of the main types of plastics (Ling et al., 2023; Ignatyev, 2014) that is used to make pipes, profiles, rigid films, cables, electric appliances, containers, carrier bags, etc. (J. Zhang et al., 2023; Shinohara and Uchino, 2020). In recent years, the enormous usage of short-lived PVC plastic products has led to tremendous growth in waste PVC (WPVC) (Dong et al., 2023; Y. Liu et al., 2020; Meng et al., 2021). PVC products may have a lifetime between one year to one hundred years, depending on the industry in which they are used (Y. Liu et al., 2020; Torres et al., 2020). This results in a disproportion between the amount of waste and the consumption rate. It is crucial to make significant efforts in creating sustainable alternatives and improving recycling technologies in order to reduce the environmental consequences of plastic waste and establish a more balanced consumption system in the future (Ghalandari et al., 2023).

The traditional approach to waste plastic disposal primarily involves landfills. Landfills are designated disposal sites for various types of waste, including household, commercial, and industrial materials. Landfills remain a significant environmental concern due to potential pollution and long-term management challenges (Y. Zhang et al., 2022; Geng et al., 2022). Leaching of chlorine, phthalate, and heavy metals from WPVC in landfills poses a serious threat to terrestrial and aquatic ecosystems (Du and Li, 2023; Hosseini et al., 2023). The other method of disposing WPVC is incineration with energy recovery. Incineration is a waste treatment process that involves the combustion of organic substances contained in waste materials. It is typically used to reduce the volume of waste and to generate energy in the form of heat or electricity (De et al., 2020; M. Shen et al., 2021). However, the chlorine in WPVC polymers during incineration might cause dioxin emissions, equipment damage due to high halogen content, and a decline in efficiency (Kim et al., 2008; Z. Xu et al., 2020; Peng et al., 2022). As a result, the chlorine should be removed from WPVC before energy recovery or chemical upcycling (Ling et al., 2023). Hydrothermal treatment (HTT) is a process used for the treatment of organic materials, such as biomass and certain types of waste like plastic. In HTT, the organic materials are subjected to

temperatures typically ranging from 150 °C to 350 °C and pressures ranging from 5 to 30 MPa (megapascals) in the presence of water (Ghalandari, 2023). HTT has recently been presented as a viable approach for the dechlorination of WPVC (Ling et al., 2023; Poerschmann et al., 2015a; Gandon-Ros et al., 2020; Ma et al., 2021; M. Yang et al., 2021; Ghalandari et al., 2022). WPVC may be hydrothermally dechlorinated at moderate temperatures and short residence times without the production of gaseous organochlorines (Takeshita et al., 2004; Y. Shen, 2020). Between 250 and 350 °C, chlorine in WPVC may be eliminated mostly as HCl in process liquid through HTT under an inert environment (Ghalandari et al., 2022; Čolnik et al., 2022). In addition, water is an eco-friendly solvent that is advantageous for purification, separation, and recovery (Bhat et al., 2020; Lu et al., 2022; Duangchan et al., 2023).

It has been demonstrated that acids have the ability to improve the HTT process (Choi et al., 2015; Bi et al., 2022; Chandrasekar et al., 2022; X. Xu et al., 2023; Sarrion et al., 2022). For instance, the influence of different acids on the HTT (AHTT) of municipal sewage sludge was studied (R. Liu et al., 2018). The findings demonstrated that acid pretreatment boosted the yield of HTT. Citric acid, a naturally occurring organic acid, has been suggested as a reagent to use in the HTT of PVC because it accelerates dechlorination by supplying hydroxyl ions (Wei et al., 2022). One research reported that citric acid enhanced the dechlorination of PVC (Lu et al., 2020) through HTT at 260 °C and 1 h. Based on the results, the dechlorination efficiency (DE) was achieved as high as 87.20% at a pH of 5. Another study presented an HTT of PVC and pomelo peel at 220 °C and 6 h using citric acid as a solvent. The study explores the potential of this approach for producing hydrochar with desirable properties. The results revealed that the resulting hydrochar had an adequate HHV (22.58 MJ/kg), energy yield (51.76%), and DE (90.50%) (Wei et al., 2022). Acids, like citric acid, expedite dechlorination by supplying hydroxyl ions, enhancing dechlorination efficiency and reducing environmental impact by minimizing the release of harmful chlorine compounds. Furthermore, acids catalyze the dechlorination reaction, leading to faster kinetics and shorter reaction times (Ghalandari, 2023). One of the main obstacles to using acids in the HTT process is their high price in comparison to water. Acids are often non-recoverable and excess acids are often found in HTT process liquid resulting in a higher HTT operating cost. Therefore, it is necessary to find a cheaper source of acid in order to use it in the HTT process.

Therefore, this research aimed to examine the possibility of using an acidic hydrothermal carbonization (HTC) process liquid in place of water in the HTT in order to dechlorination of WPVC. The primary advantage of using an acidic process fluid (PF) in the HTT might be reducing the harmful effect of disposing of it to the environment. The second advantage is saving fresh water in the HTT process because HTT process requires water (often 10 times to the waste) (Islam et al., 2022). In this work, a PF obtained from HTC of orange peel was employed to enhance the dechlorination of WPVC during HTT. AHTT experiments were performed in three temperatures (300, 325, and 350 °C), and five residence times (0.25, 0.5, 1, 2 and 4 h). Finally, several analyses were performed to characterize the resulting char and crude oil from AHTT. The novelty of this research is based on the impact of PF on the dechlorination of WPVC, and the possibility of producing solid and liquid fuels from WPVC using the AHTT process. This research breaks new ground by investigating the use of an acidic HTC process fluid (PF) as a replacement for water in the HTT for dechlorination of WPVC, potentially reducing the environmental impact of both WPVC and HTC process liquid disposal, and by investigating the possibility of producing a clean solid and liquid fuels from WPVC using the AHTT process.

2. Material and methods

2.1. Material

PVC tube was acquired from a local store as a WPVC for this study. The dichloromethane (DCM) with a purity level of 99.5% and the $\rm N_2$ gas with a purity level of 99.9% was acquired from Fisher Scientific in Waltham, Massachusetts, and the $\rm N_2$ gas with a purity level of 99.9% was acquired from NexAir in Melbourne, Florida. Nitric acid with a concentration of 65% and hydrogen peroxide with a 30% concentration were purchased from Fisher Scientific in Waltham, Massachusetts, which were used to dissolve solid samples.

2.2. Acidic hydrothermal treatment (AHTT) method

A 100 mL Hastelloy C batch reactor made by Parr Instrument Company (model 4523HP, Moline, IL) was used for performing AHTT experiments. The reactor was heated by an electrical heater at a rate of 10 °C/min 4.0 \pm 0.1 g of WPVC powder and 40 \pm 0.1 PF were used in each experiment to obtain a mass ratio of 1–10 (WPVC to PF). As mentioned, the HTC of orange peel was performed at 260 °C, and 1 h in a 300 mL Parr reactor to produce the PF. The same procedure of one HTC of orange peels research (Espro et al., 2021) was used to generate PF with a pH of 4.2. PF was filtered by a filter with pore size of 0.1 μm to separate the solid particle.

The 100 mL reactor was purged with $\rm N_2$ gas to remove any air that may have remained in the headspace. The AHTT experiments were performed at three temperatures (300, 325, and 350 °C), and five residence times (0.25, 0.5, 1, 2, and 4 h) using PF as solvent. A control run also was performed at 325 °C and 1 h using DI water. When residence time was completed, the reactor vessel was immediately cooled using a water bath, and the gaseous product was vented in a fume hood. A vacuum filtration system was used for separating the AHTT process fluid from the AHTT char. DCM was used to dissolve crude oil in order to separate it from the aqueous phase. An electrical oven was used to dry char sample at 110 °C for 24 h. The solid yield (SY) was calculated using an equation as follows (Islam et al., 2021):

$$SY (wt\%) = \left(\frac{\text{Mass of dried solid after AHTT}}{\text{Mass of dried feedstock}}\right) \times 100\% \tag{1}$$

To minimize experiment error, all experiments were replicated, and the average with standard deviation is provided in this manuscript. As the focus of this research was on the char sample and crude oil, the gaseous product was not further investigated.

2.3. Characterization of the AHTT's char samples

The HHV of char samples was calculated using the ASTM D240 method (Islam et al. 2021) and an IKA C 200 bomb calorimeter (Stauffen, Baden-Württemberg, Germany). Before the analysis, 0.5 g of the material was dried for 12 h at $105\,^{\circ}$ C. Using the ASTM D 1102 technique (Reza et al., 2013a), the ash content of the solid sample was determined. The HHV findings were reported on a basis of dry weight. The following formula was used to calculate the energy yield, EY (%) (Islam et al. 2021):

EY (%) = SY (wt%)
$$\times \frac{\text{HHV of dried char product}}{\text{HHV of dried feedstock}}$$
 (2)

Using a CHNS analyzer, the N, H, C, and S content of AHTT solid products were determined (Thermo FLASH EA 1112 Series). The analysis was done according to ASTM D5373 standard (Islam et al. 2021). Vanadium pentaoxide was used as a conditioning agent, and 2, 5-Bis (5-tert-butyl-benzoxazol-2-yl) thiophene was used as a calibration standard (Quaid et al., 2022). Each sample was burnt in oxygen at 950 °C (the carrier gas was helium). A difference method was used to determine the O content.

PerkinElmer's TGA 4000 thermogravimetric analyzer (Waltham, MA, USA) was used to quantify the fixed carbon (FC) and volatile matter (VM) of solid samples. In order to avoid any kind of oxidation process and purge the VM at the same time, a steady flow of N_2 gas (40 mL/min) was utilized throughout the analysis. The char sample was originally heated to 110 °C at a rate of 20 °C/min, and then an isothermal state was maintained for 5 min. In the second phase, the sample was heated to 900 °C at a rate of 20 °C/min before being held in an isothermal atmosphere for 10 min. Based on the quantity of mass lost between 110 and 900 °C, the VM was calculated. FC was ultimately calculated using the difference between VM and ash.

Using an energy dispersive X-ray (EDX) analyzer, the semi-quantitative inorganic composition of ash samples was measured (Octane plus, EDAX, USA). All samples were coated with gold using Denton Vacuum Desk III vacuum sputtering equipment (Moorestown, NJ, USA). Several correlations were applied to analyze the slagging/fouling tendency based on the composition of ash samples (Tortosa Masiá et al., 2007). On the basis of Table S1, the slagging, fouling, alkali, ratio-slag, and Cl contents were estimated. The correlations take the form B/A, where B represents low melting point chemicals (CaO + Cr₂O₃ + Fe₂O₃ + Mo₂O₃ + WO₂) and A represents high melting point compounds (SiO₂ + TiO₂ + Ni₃O₄ + Al₂O₃).

The attenuated total reflector (Nicolet iS5) from Thermo Scientific was used to determine the functional groups contained in solid materials (Madison, WI, USA). The resolution was set to 4 cm⁻¹, the data accumulation to 64, and the wavenumber range to 400–4000 cm⁻¹.

Using a Dionex Aquion IC (ion chromatography) system (Thermo Scientific), the chlorine concentration in the (dissolved) solid product and the aqueous phase was determined. The process of digestion was employed to create the liquid injection sample from the solid product (Pettersson and Olsson, 1998). For digestion, nitric acid (2 mL) and solid product (10 mg) were introduced to a chemical volumetric flask. The combination was heated for 60 min at 80 °C using an electrical heater. Then, it cooled down to reach ambient temperature. The mass loss that happened during digestion was recorded. 2 mL of hydrogen peroxide was then added. Following a further 60 min of heating at 80 °C, the combination cooled down to ambient temperature. The combination was then diluted with DI water to prepare the sample for injection into IC in order to assess the char's chlorine level. To evaluate the chlorine concentration in the aqueous phase, the phase was diluted with DI water and injected into IC. The following equation was applied for the purpose of determining DE (Ghalandari et al., 2023):

DE (%) =
$$\frac{C_1 - C_2}{C_1} \times 100$$
 (3)

where C_1 and C_2 indicate the chlorine mass of the feedstock and char sample (in a dry mass basis), respectively.

The combustion test was conducted using the PerkinElmer TGA 4000 thermogravimetric analyzer (Waltham, Massachusetts, United States). 5–10 mg of the material was placed in a crucible, while 40 mL/min of air was continually blasted through it. In three phases, the temperature raised from 30 to 900 °C: 35 °C for 10 min, 110 °C for 5 min, and 900 °C at a rate of 20 °C/min. The distinctive characteristics of the combustion test are the beginning weight loss temperature, indicated by $T_{\rm i}$, the burnout temperature, denoted by $T_{\rm f}$, the maximum burning rate, represented by DTG_{max}, and the average burning rate, denoted by DTG_{mean}. S, the complete combustion index, was computed using the following equation (D. Zhao et al., 2016):

$$S = \frac{DTG_{max} \times DTG_{mean}}{T_i^2 \times T_f}$$
 (4)

2.4. Characterization of AHTT's crude oils

A Thermo Flash 1112 Elemental Analyzer was utilized for ultimate analysis (Waltham, MA, USA). The required AHTT's crude oil was

separated from DCM by natural convection in an aluminum sample pan. About 9.75 \pm 0.25 mg of vanadium pentoxide was mixed with 2.0 \pm 0.5 mg of AHTT's crude oil without DCM. The elemental analyzer analyzed C, H, sulfur, and N, while elemental O was determined using the difference technique. Using the Dulong formula (Seshasayee and Savage, 2020), the HHV of AHTT's crude oil was determined.

HHV (MJ / kg) =
$$0.3383 \text{ C} + 1.422 \left(H - \frac{O}{8}\right)$$
 (5)

Using a PerkinElmer TGA 4000, the boiling point (BP) distributions of the AHTT's crude oil was specified (Waltham, MA, USA). TGA analysis was performed in an inert atmosphere with an $\rm N_2$ flow rate of 20 mL/min (Banivaheb et al., 2022). The AHTT's crude oil was heated to 40 °C from 25 °C and maintained under isothermal conditions for 10 min to remove any remaining DCM. The temperature was then increased from 40 to 600 °C at a rate of 20 °C/min. The sample was kept isothermally at 600 °C for 5 min before the heating was stopped (Ghalandari et al., 2022).

A Nicolet 6700 FTIR Spectrophotometer was utilized to characterize AHTT's crude oil (Waltham, MA, USA). The range of scanned spectra between was 500 and 4000 cm⁻¹ to identify the functional groups in AHTT's crude oil. Because the AHTT's crude oil and DCM were mixed, a drop of the mixture was placed on an IR card for 5 min to allow the DCM to evaporate spontaneously. Then, the FTIR analysis was undertaken in the following context: Transmittance mode, data accumulation: 64, resolution: 4 (Ghalandari et al., 2024).

Using an Agilent 7890 GC equipped with a 5975 Mass Spectrometric Detector, mass spectrometric gas chromatography analyses were conducted. The GCMS had a Supelco Equity 1701 column. An intake temperature of 250 $^{\circ}\text{C}$ was maintained using a split ratio of 1:1 and a helium flow rate of 5 mL/min. The oven was heated for 20 min at a rate of 3 $^{\circ}\text{C}/\text{min}$ after being warmed to 45 $^{\circ}\text{C}$ for 4 min. AHTT's crude oil was spiked (0.1 wt%) with an internal standard (99% n-decane) without any overlapping chromatogram peaks (Ghalandari et al., 2022).

3. Results and discussion

3.1. Dechlorination of WPVC

Fig. 1 indicates that using PF has a positive effect on DE of WPVC. Based on the results, using PF instead of water improves the DE from 90.33 to 95.37% at 325 °C, and 1 h. The acidic nature of the PF enhances the dechlorination process by catalyzing the cleavage of carbon-chlorine (C–Cl) bonds in WPVC molecules. This catalytic effect accelerates the breakdown of PVC polymer chains, leading to more efficient removal of chlorine atoms from the polymer structure (Ghalandari et al., 2022). AHTT temperature has a significant effect on chlorine elimination, as the

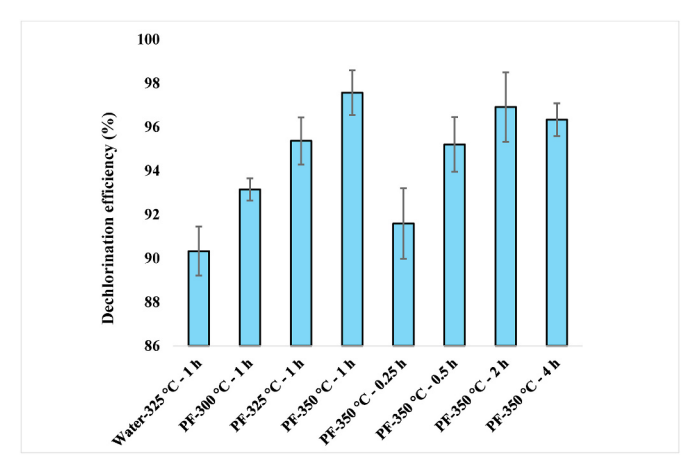


Fig. 1. The DE of WPVC at different AHTT conditions.

DE increases from 93.15% at 300 °C to 97.57% at 350 °C (for 1 h). It shows that the bulk of the chlorine in WPVC can be removed by the AHTT at 350 °C and 1 h, although some amount of chlorine is still present in the char samples. These remaining organic chlorine atoms may be carbon atoms with sp²-hybridization in olefinic and aromatic structures that are resistant to the process of nucleophilic substitution (Poerschmann et al., 2015b). As shown in Fig. 1, by extending the AHTT time from 0.25 to 1 h at 350 °C, the DE rises from 91.59 to 97.57%; however, it decreases to 96.33% when the AHTT time is increased to 4 h. This outcome is consistent with earlier HTT dechlorination results in the scientific literature (Y. Zhao et al., 2022; Li et al., 2017). This might be explained by the carbonization and pore generation that occur during higher residence times, increasing the capacity of char samples for adsorption. As a consequence, some of the dissolved chlorine in the aqueous phase may be adsorbed onto the char samples, leading to a reduction in DE (Y. Zhao et al., 2022).

Table 1 displays chlorine distribution in the solid and aqueous phases at various AHTT conditions. Regardless of the AHTT condition, the chlorine in WPVC undergoes a substantial reduction through AHTT. Literature also reported the majority portion of chlorine of PVC moves from solid phase to aqueous phase during HTT, and chlorine does not exist in gas phase (Takeshita et al., 2004; Poerschmann et al., 2015a). As shown in Table 1, a small fraction of chlorine is lost during sample collection in addition to measurement errors (P. Zhao et al., 2017). The chlorine concentration of char samples drops from 564.5 (g/kg) to 56.60 (g/kg) during HTT (control run), and from 564.5 (g/kg) to 26.16 (g/kg) during AHTT at 325 °C, 1 h. The aqueous phase's pH drops from 6.4 to 1.78 for HTT and from 4.2 to 0.86 AHTT at 325 °C, 1 h which indicates the production of significant amount of HCl. The minimum amount of char's chlorine content (13.73 g/kg) and minimum pH of the aqueous phase (0.67) are achieved for AHTT at 350 °C, 1 h. These findings underscore the effectiveness of AHTT, particularly at elevated temperature (350 °C) and optimum reaction time (1 h), in promoting acid-catalyzed dechlorination reactions, thereby reducing PVC content and generating HCl. The DE results of the current study are compared with those of previous studies in Table 2.

Fig. 2a depicts the FTIR spectra of the functional groups of WPVC, and two char samples (Water-325 $^{\circ}\text{C-1}$ h, and PF-325 $^{\circ}\text{C-1}$ h). The remaining FTIR spectra of char samples are presented in Fig. S1. For WPVC, strong transmittance bands at around 610 and 850 cm⁻¹ are due C-Cl stretching vibrations (Li et al., 2017). The transmittance bands at around 2915, 1253, and 1099 cm⁻¹ are attributed to the C-H, Cl-C-H, and C-C stretching vibrations, respectively (Li et al., 2017; Lv et al., 2009). The transmittance band at about 1253 cm⁻¹, which corresponds to skeletal vibration Cl-C-H, and the transmittance bands at 850, and 610 cm⁻¹, which related to the C–Cl bending vibration nearly vanish. It can be seen from Fig. 2a that the AHTT breaks the skeletal chain and removed most of the chlorine from WPVC (Yoshioka et al., 2008; Li et al., 2017). The peaks at 1629 and 3379 cm⁻¹, which related to the C=C and O-H stretching vibrations appear in char samples. This result is in line with the ultimate analysis. As shown in Fig. 2b, there are two possible routes for dechlorination: elimination and substitution. The elimination procedure begins with the formation of chloroallylic compounds and free radicals, accompanied by the elimination of HCl to generate polyenes (Y. Shen, 2016). Then, the allyl chlorine atom on the carbon atom would dissociate into -Cl and -H, forming two double bonds. The peak at 1629 cm⁻¹ for char samples supports this theory by showing how the zipper mechanism fulfills the dehydrochlorination process by activating subsequent chlorine molecules (Poerschmann et al., 2015b; Ma et al., 2019). This peak, which appears after AHTT and coincides with a rise in the strength of C=C stretching vibrations, shows that HCl is removed from WPVC after AHTT. Regarding substitution, one simple way is to substitute the -Cl with -OH. The second way is to substitute both the -H and -Cl with two -OH. Then, intramolecular and intermolecular dehydration would take place, producing H₂O and HCl. The peaks detected at 3379 cm⁻¹ are ascribed to the O-H stretching

Table 1The chlorine balance and pH of the aqueous phase after AHTT.

Sample	Cl in solid (%)	Cl in aqueous (%)	^a Error (%)	Cl in solid (g/kg)	Cl in aqueous (g/l)	pH of aqueous phase
WPVC	100 ± 0.00	_	_	564.50	_	_
Water-325°C-1h	9.67 ± 1.69	89.45 ± 2.62	0.88	56.60	50.49	1.78 ± 0.13
PF-300°C-1h	6.85 ± 1.22	88.58 ± 3.21	4.57	38.69	50.00	1.02 ± 0.07
PF-325°C-1h	4.63 ± 1.22	92.25 ± 1.98	3.12	26.16	52.08	0.86 ± 0.05
PF-350°C-1h	2.43 ± 0.87	93.36 ± 1.52	4.21	13.73	52.70	0.67 ± 0.04
PF-350°C-0.25 h	8.41 ± 2.75	86.21 ± 4.21	5.38	47.46	48.67	0.95 ± 0.02
PF-350°C-0.5 h	4.80 ± 1.85	91.39 ± 3.35	3.81	27.08	51.59	0.82 ± 0.02
PF-350°C-2h	3.09 ± 1.68	92.35 ± 2.89	4.56	17.43	52.13	0.70 ± 0.06
PF-350°C-4h	3.67 ± 0.77	90.85 ± 0.95	5.48	20.71	51.28	0.75 ± 0.07

^a Error (%) = 100 - Cl in aqueous phase (%) – Cl in solid phase (%).

Table 2Dechlorination efficiency (DE) of PVC throught hydrothermal treatment (HTT) for different additive and operational conditions.

Feedstocks	Additives	Operation condition		DE (%)	Refs
		T (°C)	t (min)		
PVC	-	250	30	76.4	Endo and Emori (2001)
PVC	_	300	60	~80	Takeshita et al.
		350	60	~90	(2004)
PVC	Citric Acid	220	360	~90	Wei et al. (2022)
PVC	Citric Acid	260	60	~87	(Lu et al., 2020)
PVC	HTC process	300	60	93.15	Current study
	fluid (PF)	325	60	95.37	
		350	60	97.57	
PVC	Sodium	225	1440	~90	Shin et al. (1998)
	hydroxide	250	300	100	
PVC	Sodium	220	120	~90	Ma et al. (2002)
	hydroxide	260	120	~90	
PVC	Sodium	220	30	76.74	Li et al. (2017)
	hydroxide	240	60	94.3	
PVC	Ammonia	230	60	~90	(Hashimoto et al.,
		230	120	~75	2008)
		230	120	~90	
PVC	Ammonia	210	60	65.2	Xiu et al. (2020)
		250	60	94.8	
		300	60	98.7	

vibration, which is clearly enhanced in char samples. This finding shows the substitution reaction play a main role on dechlorination of WPVC.

3.2. Physicochemical properties of AHTT's chars

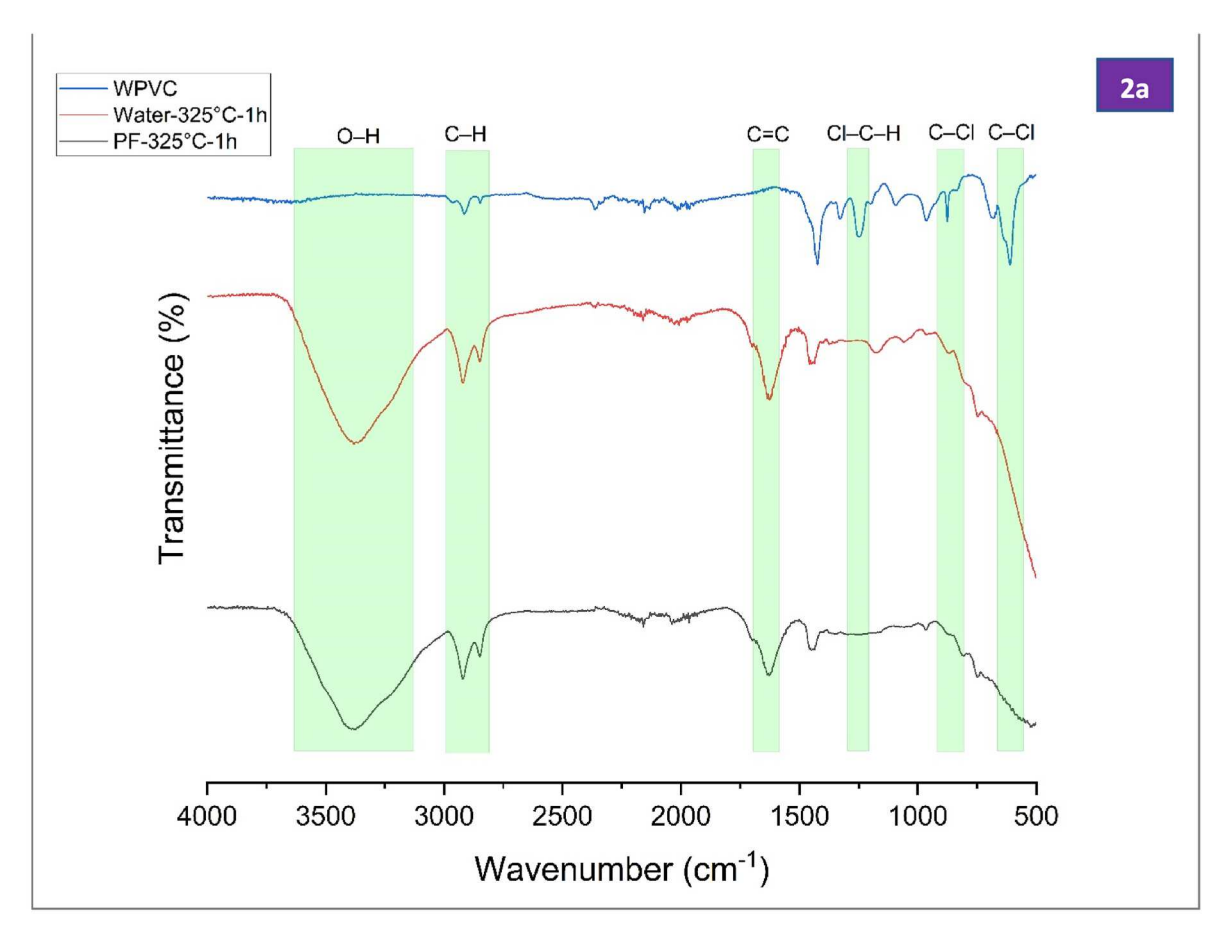
The solid yield for various AHTT conditions is illustrated in Table 3. The solid yield for the control run, is 64.44% at 325 °C and 1 h. Results illustrate that solid yield decreases significantly from 64.44% to 54.27% at 325 °C for 1 h by replacing water with PF. One research showed that solid yield decreased by utilizing acids as the reagent through HTT (W. Yang et al., 2014). A similar solid yield trend was observed when organic and inorganic acids were used in the HTT of biomass (Zou et al., 2009; Ross et al., 2010). The decrease in solid yield is likely due to the acidic nature of the PF, which alters the chemical environment and promotes increased degradation of the WPVC material, resulting in shorter polymer chains and reduced solid yield (Ghalandari et al., 2023).

As can be seen in Table 3, the AHTT temperature has a considerable impact on the WPVC conversion since the solid yield decreases from 56.88% at $300\,^{\circ}\text{C}$ to 49.85% at $350\,^{\circ}\text{C}$. it demonstrates that the reaction severity increases from 300 to $350\,^{\circ}\text{C}$; therefore, a higher temperature is more significant to convert the WPVC into the polymer with shorter chains. One acidic HTT study reported that the highest solid conversion is obtained at $350\,^{\circ}\text{C}$ (Zou et al., 2009). Table 3 further illustrates that by extending AHTT time from 0.25 to 1 h, the solid yield decreases significantly from 60.92 to 49.85% at $350\,^{\circ}\text{C}$; however, the solid yield

increases slightly from 49.85% for 1 h to 52.8% for 4 h at 350 $^{\circ}$ C. A previous study reported a similar change in solid yield with HTT time (Ross et al., 2010). This might be because of the competition between repolymerization reaction, and hydrolysis reaction, which are two liquefaction-related reactions. During AHTT, the WPVC is initially broken down and turned into shorter polymer chains, but when the AHTT time is prolonged, the polymerization, cyclization, and condensation process may ultimately rearrange them to generate solid residues (Ross et al., 2010).

Table 3 displays the findings of ultimate and proximate analysis performed on WPVC and char samples to evaluate the variation in the composition of elements and fixed carbon/volatile content. By evaluating the results, it can be found that the AHTT has a significant effect on the volatile matters (VM) and fixed carbon (FC). The VM of the char samples drops from 56.45 to 50.48 wt%, and the FC of the char samples raises from 33.69 to 39.84 wt% by using PF instead of water at 325 °C and 1 h. By extending the AHTT temperature from 300 to 350 °C at 1 h, the VM of char samples drops from 52.36 to 47.44 wt%, and the FC of the char samples raises from 38.66 to 45.67 wt%. Moreover, by extending the AHTT time from 0.25 to 4 h at 350 $^{\circ}\text{C}$, the VM of char samples drops from 54.11 to 48.80 wt%, and the FC of the char samples raises from 36.19 to 47.15 wt%. The observed changes in VM and FC content of the char samples can be attributed to the alterations in reaction conditions during AHTT. Substituting water with PF or varying AHTT temperature and duration affects the thermal decomposition process of WPVC, leading to differences in the composition of the resulting char samples. Specifically, using PF or increasing AHTT temperature and duration promotes more extensive thermal degradation of WPVC, resulting in a reduction in VM and an increase in FC content in the char samples. Literature also reported that by raising the HTT temperature, the VM content and the FC content of the char sample decreased and increased, respectively (Zou et al., 2009; Yao and Ma, 2018).

Table 3 illustrates that char samples possess a higher C and H contents in compared to WPVC. Using PF instead of water at 325 °C and 1 h raises the C content of the char samples from 64.85 to 68.59 wt% and the H content from 6.24 to 6.76 wt%. Therefore, as can be seen in Fig. 3 (3a), the O/C atomic ratio reduces, and H/C atomic ratio increases. When AHTT temperature is increased from 300 to 350 °C at 1 h, C content increases significantly from 61.55 to 75.19 wt%, H content raises from 5.58 to 7.82 wt% and O content drops from 8.79 to 5.14 wt%. Thus, increasing AHTT temperature reduces the O/C atomic ratio and raises the H/C atomic ratio. When AHTT time is increased from 0.25 to 4 h at 350 °C, C content raises significantly from 62.02 to 76.82 wt%, H content raises from 5.91 to 8.45 wt% and O content drops from 8.39 to 3.70 wt%. As a result, the O/C atomic ratio decreases, and H/C atomic ratio increases by increasing AHTT time. Substituting water with PF, increasing AHTT temperature, and extending AHTT time promote more extensive thermal degradation of WPVC, resulting in increased C content and H content in the char samples. Notably, S concentration is negligible for char samples. The N concentration was lower than the ultimate analyzer's detection limit. Similar results for S and N concentrations were



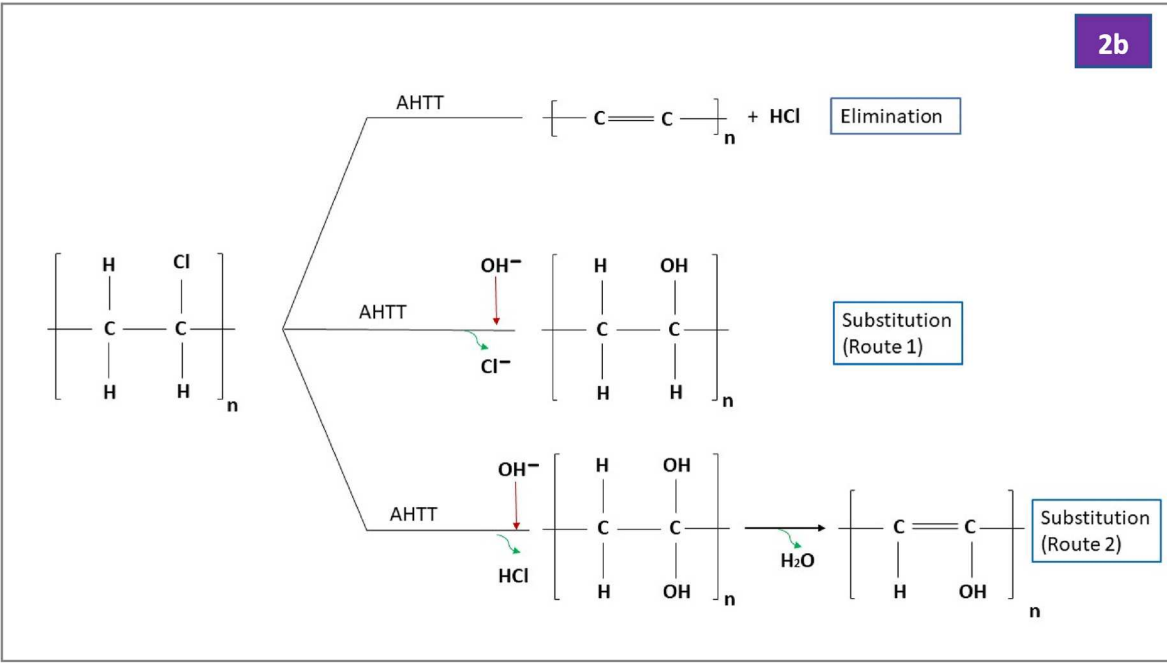


Fig. 2. (2a) FTIR analysis of the WPVC, and two char samples produced (Water-325 °C-1 h, and PF-325 °C-1 h), (2b) chemical reaction mechanism for dechlorination of WPVC through AHTT (Adapted from literature (P. Zhao et al., 2017; Ma et al., 2021).

reported in the literature (Yao and Ma, 2018).

3.3. Fuel and combustion properties of AHTT chars

Fig. 4 illustrates that the char samples have higher HHV in compared

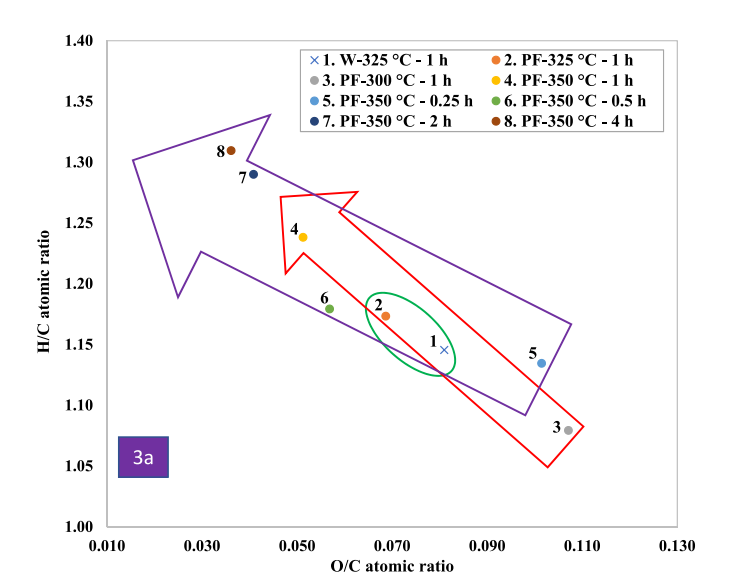
to WPVC, that is because of higher C and H contents in char samples. The HHV of char sample raises from 25.14 to 27.30 MJ/kg by using PF instead of water; Nevertheless, EY decreases from 79.62 to 72.81%. When AHTT temperature is raised from 300 to 350 $^{\circ}\text{C}$ at 1 h, the HHV rises noticeably from 22.77 to 31.26 MJ/kg MJ/kg, and EY rises from

Table 3
Solid yield, proximate and ultimate analysis for WPVC, and char samples produced at different AHTT conditions.

Sample	Solid yield (wt%)	Proximate analysis ^a		Ultimate analysis ^a					
		VM (wt%)	FC ^b (wt%)	Ash (wt%)	C (wt%)	H (wt%)	S (wt%)	O ^c (wt%)	Cl (wt%)
WPVC	_	86.44 ± 1.55	10.35	_	34.79 ± 1.34	4.08 ± 1.65	0.37 ± 0.03	-	56.45 ± 3.35
Water-325°C-1h	64.44 ± 1.21	56.45 ± 0.89	33.69	9.86 ± 0.12	64.85 ± 2.12	6.24 ± 0.24	BD	7.00	$12.05~\pm$
PF-300°C-1h	56.88 ± 2.42	52.36 ± 0.53	38.66	8.98 ± 1.15	61.55 ± 1.32	5.58 ± 0.35	0.09 ± 0.05	8.79	15.01 ± 0.85
PF-325°C-1h	54.27 ± 1.31	50.48 ± 1.32	39.84	9.68 ± 0.92	68.59 ± 2.89	6.76 ± 0.42	0.15 ± 0.04	6.28	$\textbf{8.54} \pm \textbf{0.40}$
PF-350°C-1h	49.85 ± 1.81	47.44 ± 1.21	45.67	6.89 ± 1.21	75.19 ± 0.78	$\textbf{7.82} \pm \textbf{0.64}$	0.08 ± 0.02	5.14	4.88 ± 0.62
PF-350°C-0.25 h	60.92 ± 2.80	54.11 ± 2.02	36.19	9.70 ± 1.20	62.02 ± 1.62	5.91 ± 1.02	0.18 ± 0.03	8.39	13.8 ± 0.24
PF-350°C-0.5 h	55.92 ± 0.95	51.70 ± 0.56	41.33	6.97 ± 0.91	71.78 ± 2.18	7.11 ± 0.44	0.12 ± 0.01	5.44	8.58 ± 1.2
PF-350°C-2h	51.62 ± 1.92	48.62 ± 0.75	46.02	5.36 ± 0.43	76.23 ± 1.54	8.26 ± 1.80	0.02 ± 0.01	4.15	5.98 ± 1.20
$PF\!-\!350^{\circ}C\!-\!4h$	52.80 ± 0.84	48.80 ± 0.98	47.15	4.05 ± 0.52	76.82 ± 1.32	8.45 ± 1.50	0.03 ± 0.01	3.70	6.95 ± 0.54

^aDry basis.

^dBD: Below detection limit.



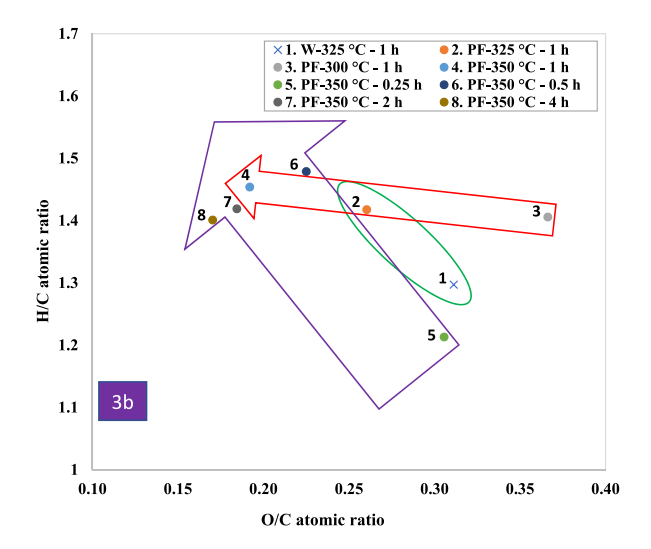


Fig. 3. Van Krevelen diagram of char samples (3a) and crude oils (3b) created at different AHTT conditions (green oval: impact of using PF instead of water, purple arrow: impact of AHTT time, red arrow: impact of AHTT temperature).

63.63% to 76.57%. The HHV rises from 23.48 to 33.07 MJ/kg when the AHTT time is raised from 0.25 to 4 h at $350\,^\circ\text{C}$, indicating that the AHTT time has a beneficial effect on the HHV. Extending AHTT time causes a

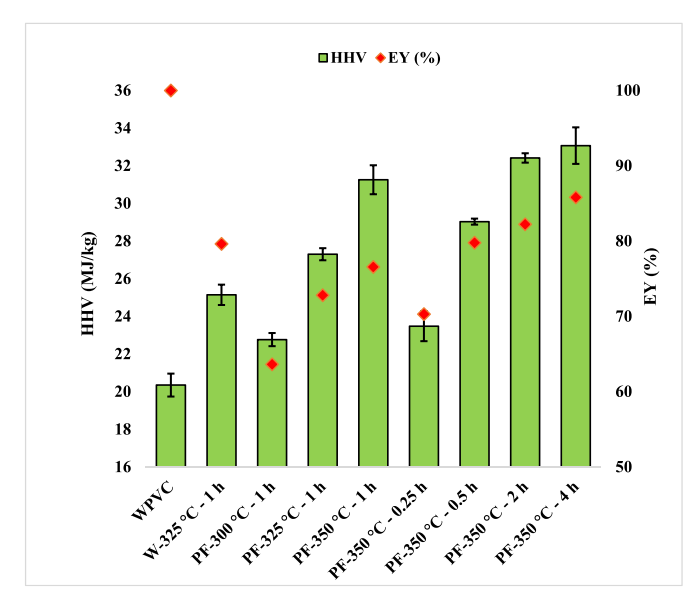


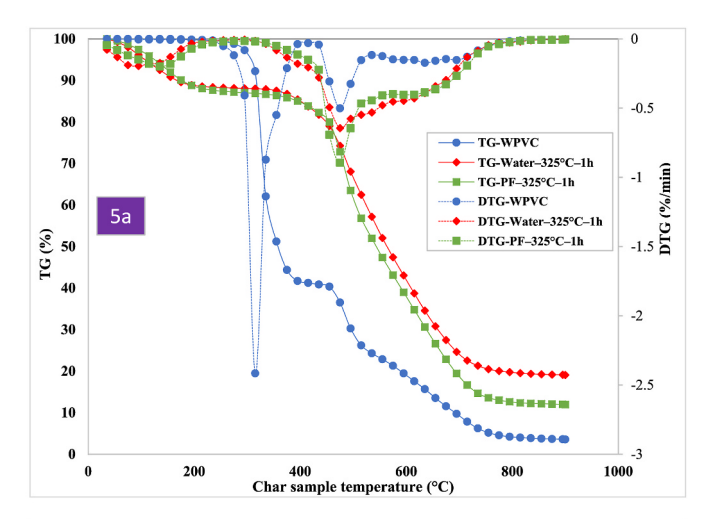
Fig. 4. Higher heating value (HHV) and energy yield (EY) for WPVC, and char samples produced at various AHTT conditions.

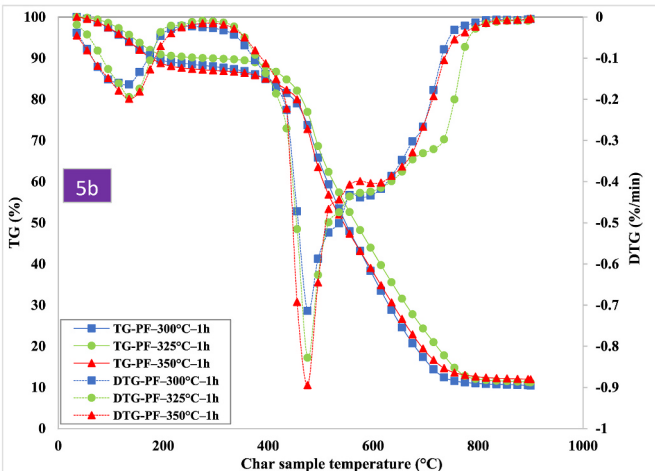
fluctuation in the EY; however, overall, it increases from 70.29 to 85.80% when AHTT time is increased from 0.25 to 4 h. The char sample at 350 $^{\circ}$ C, and 4 h has maximum HHV (33.04 MJ/kg) and EY (85.80%). The dehydrochlorination process, which involves the removal of chlorine atoms from the PVC polymer chains, is the main mechanism responsible for the increase in C and H contents observed during the AHTT of WPVC. This dehydrochlorination reaction leads to the removal of chlorine atoms from the PVC polymer structure, thereby increasing the relative proportions of C and H in the resulting char samples (Yao and Ma, 2018).

The combustion characteristics of WPVC and char samples were evaluated using TGA. The TG and DTG curves of WPVC and char samples are shown in Fig. 5. The DTG curve for WPVC includes two main peaks. The strong peak with a weight loss of 54.7% corresponds to the dehydrochlorination reaction (between 273 and 397 °C). The next peak with a weight loss of 15.9% is related to the combustion of VM and FC (between 441 and 519 °C). The combustion of char samples includes one part, demonstrating that AHTT improved the uniformity of the solid. Since there are fewer CH–Cl bonds in the char samples in comparison to WPVC; therefore, there is not a peak for dehydrochlorination reaction in DTG curve of char samples in contrast to WPVC. Using PF instead of water leads to a more mass loss in TG curve and a sharper peak in DTG curve, resulting a faster burning rate (Wang et al., 2018). The acidity

 $^{{}^{}b}FC \text{ (wt\%)} = 100 - VM \text{ (wt\%)} - Ash \text{ (wt\%)}.$

 $^{^{}c}O(wt\%) = 100 - C(wt\%) - H(wt\%) - N(wt\%) - S(wt\%) - Cl(wt\%) - Ash(wt\%).$





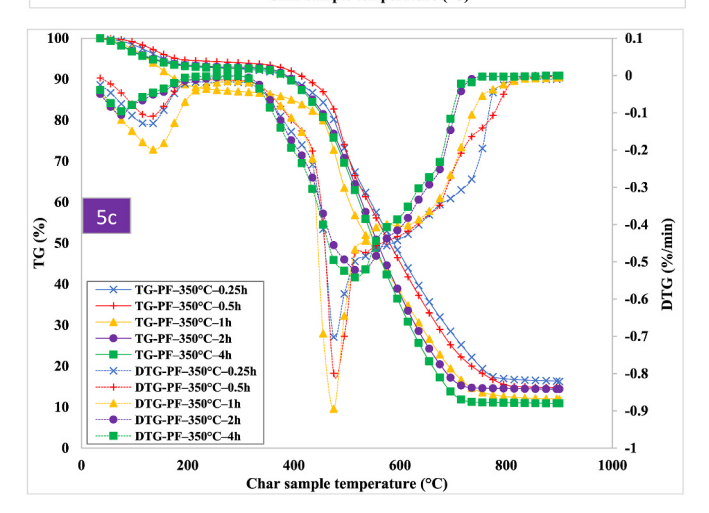


Fig. 5. TG-DTG curves for WPVC, and char samples produced at various AHTT conditions. (5a. effect of water and PF, 5b. effect of AHTT temperature, 5c. effect of AHTT time).

enhances the degradation of WPVC during AHTT, resulting in more efficient release of volatile components and faster combustion rates (Ghalandari et al., 2023). Increasing AHTT temperature has no significant effect on TG curve, but it leads to sharper peak in DTG curve. While the TG curve may not exhibit significant changes with temperature variations, the DTG curve reflects the sensitivity of the decomposition process to temperature changes, with higher temperatures leading to faster decomposition rates and sharper peaks. Increasing AHTT time

from 0.25 to $4\,h$ leads to a more mass loss in TGA curve, and from 0.25 to $1\,h$ lead to a sharper peak in DTG curve; however, at longer AHTT time (2 h, and 4 h), weaker peaks are observed.

Table 4 depicts combustion parameters of WPVC and AHTT char samples. As seen in Table 4, WPVC has a lower T_i (the beginning weight loss temperature) as well as higher T_f (the burnout temperature) in comparison to char samples, which shows WPVC has a wider combustion zone. The T_g (the temperature according to DTG_{max}) for WPVC happens in 315 °C but for char samples happens in the range of 475–515 °C. WPVC includes a high concentration of C–Cl bonds with weak bond energy that are susceptible to breaking at low temperatures (Wang et al., 2018). The AHTT improves the solid's T_i by eliminating chlorine, creating a carbon chain, and raising the degree of coalification (Lin et al., 2020; Ning et al., 2020).

When PF is applied in place of water, T_i of char sample increases from 375 to 395 °C and T_f increases from 735 to 755 °C, indicating that PF may drive combustion into the high-temperature zone (Lin et al., 2016). AHTT time has no effect on the combustion zone from 0.25 to 1 h but in longer AHTT time (2 and 4 h), the T_f of char samples drops from 755 to 715 °C, resulting in a shorter combustion zone.

To evaluate the performance of char samples as solid fuels, the comprehensive combustibility index (S) was calculated. A high S index indicates a more vigorous combustion reaction and is correlated with the mass loss rate. On the other hand, a high mass loss rate might lead to an unstable flame and severe energy loss (Jiang et al., 2016). It can be seen in Table 4, WPVC has a higher S index compared to char samples due to the formation of HCl during combustion, which might cause an unstable flame. The chlorine concentration of the solid reduces during AHTT; hence, the harmful effects of the generation of HCl on flame are lessened (Y. Zhao et al., 2022). Table 4 demonstrates that raising the AHTT temperature increases the combustion performance of the char sample. When the AHTT temperature is raised from 300 to 350 $^{\circ}$ C, the S index of the char samples rises from 1.26 (\times 10⁻⁹) to 1.43 (\times 10⁻⁹). The reason might be due to the development of pores in char sample structure at high temperatures (Y. Zhao et al., 2022). Furthermore, by extending AHTT time from 0.25 h to 1 h at 350 °C, the S index value increases from 1.11 (\times 10⁻⁹) to 1.43 (\times 10⁻⁹), but it drops to 0.54 (\times 10⁻⁹) for 4 h at 350 °C. The combustion is more intense in high S index, and the char samples with higher S index will burn faster (Lin et al., 2015).

3.4. Slagging and fouling indices of AHTT's chars

Important metrics used to evaluate the burning properties of fuels include the fouling index (I_F), slagging index (I_S), slag viscosity index (I_V), and alkali index (I_A). This is especially true when evaluating solid residues like char made from WPVC. Thermal efficiency is affected by fuel ash's tendency to settle on heat transfer surfaces inside combustion

Table 4The combustion characteristic parameters of WPVC, and char samples produced at various AHTT conditions.

Sample	T _i ^a (°C)	T _f ^b (°C)	Tg ^c (°C)	DTG _{max} (min/%)	DTG _{mean} (%/min)	^b S (10 ⁻⁹ . min ⁻² . C ⁻³)
WPVC	275	775	315	-2.42	-0.17	7.06
Water-325°C-1h	375	735	475	-0.64	-0.19	1.16
PF-300°C-1h	395	755	475	-0.71	-0.18	1.26
PF-325°C-1h	395	755	475	-0.83	-0.20	1.49
PF-350°C-1h	395	755	475	-0.89	-0.19	1.43
PF-350°C-0.25 h	395	755	475	-0.70	-0.19	1.11
PF-350°C-0.5 h	395	755	475	-0.80	-0.18	1.19
PF-350°C-2h	395	715	515	-0.52	-0.15	0.69
PF-350°C-4h	395	715	515	-0.54	-0.14	0.70

^a T_i, the ignition temperature.

 $^{^{\}text{b}}$ T_f, the burnout temperature.

^c T_o, the temperature according to DTG_{max}.

equipment, which is measured by the I_F . Similar to this, I_S gauges the probability that ash may condense into molten slag deposits, which can cause corrosion and obstructions in boilers and furnaces, among other operational problems. The I_V gives information on the molten slag's flow characteristics, which affect how easily it adheres to surfaces and may be removed (Ghalandari, 2023).

The I_F, I_S, I_V, I_A, and chlorine concentration for WPVC and char samples are presented in Table S1. Based on the EDX analysis results presented in Table S2, these indexes were calculated and presented in Table 5. The results demonstrate that the I_S value of WPVC is extremely high. During the AHTT, the value of I_S drops from an extremely high level to a low level. The lone exception is char sample at 300 °C and 1 h, for which the I_S value is medium. It demonstrates that increasing the AHTT temperature can increase the I_S value of char samples. Because of the lack of alkali elements, the IF and IA values for WPVC and char samples are low (Na₂O and K₂O). I_V value of WPVC and char samples are high, indicating the AHTT cannot enhance I_V index. The cause might be the ash's low SiO₂ concentration and high CaO concentration. Notably, the I_V value and chlorine concentration of char samples are greater than those of biomass-derived hydrochar (Reza et al., 2013b). The level of ash chlorine concentration for char samples at 350 °C for 0.5, 1, 2 h and 4 h is low; however, for the other char samples is medium. Consequently, AHTT can produce a clean solid fuel from WPVC s in terms of chlorine concentration.

3.5. Elemental compositional analysis of AHTT's crude oils

Ultimate analysis was performed on the crude oils to specify C, H, N, S, O and S contents. From Table 6, the C concentration ranges from 62.25 to 74.36 wt%, whereas the H concentration ranges from 6.75 to 8.86 wt%. N and S concentrations are below the thresholds of detection.

When PF is used in place of water, the C and H concentrations rise, producing crude oils with a greater HHV. According to the literature, utilizing organic acid via HTT produces crude oils with a greater HHV since it increases the C and H concentrations, and decreases the O concentration (R. Liu et al., 2018; Ross et al., 2010). Acidic conditions facilitate the breakdown of PVC polymer chains through hydrolysis and depolymerization reactions. The acidic environment breaks the bonds within the PVC polymer, releasing smaller molecules containing higher concentrations of C and H. Acidic conditions can also facilitate hydrogenation reactions, where H atoms are incorporated into the organic compounds derived from WPVC (Ghalandari, 2023). This results in an increase in the H concentration in the crude oils produced during AHTT. The C and H concentrations in crude oils are significantly affected by the AHTT temperature. As shown in Table 6, the C concentration rises from 62.25 to 72.56 wt% and the H concentration rises from 7.35 to 8.86 wt% when the AHTT temperature is raised from 300 to 350 °C at 1 h. Consequently, the HHV of crude oils rises from 26.11 to 33.84 MJ/kg. These findings indicate that higher AHTT temperature improves the crude oil's quality. Presumably, the viscosity of PF decreases at high AHTT temperature (350 °C), which can cause an increase in PF diffusivity into WPVC and a greater degree of conversion (Mahesh et al.,

Table 5Slagging, fouling, alkali, and ratio-slag indices, and Cl concentration of char samples ash.

Sample	I_S	I_F	I_A	I_V	Cl
WPVC	Extremely high	Low	Low	High	Extremely high
Water-325°C-1h	Low	Low	Low	High	Medium
PF-300°C-1h	Medium	Low	Low	High	Medium
PF-325°C-1h	Low	Low	Low	High	Medium
PF-350°C-1h	Low	Low	Low	High	Low
PF-350°C-0.25 h	Low	Low	Low	High	Medium
PF-350°C-0.5 h	Low	Low	Low	High	Low
PF-350°C-2h	Low	Low	Low	High	Low
PF-350°C-4h	Low	Low	Low	High	Low

Table 6Elemental composition, and HHV of crude oils at various AHTT conditions.

Sample	Carbon (wt %)	Hydrogen (wt %)	Oxygen ^a (wt %)	HHV ^b (MJ/ kg)
Water-325°C-1h	65.62 ± 0.25	7.15 ± 0.24	27.23	27.53
PF-300°C-1h	$62.25 \pm \\1.28$	$\textbf{7.35} \pm \textbf{0.24}$	30.40	26.11
PF-325°C-1h	$68.20 \pm \\ 0.41$	$\textbf{8.12} \pm \textbf{0.16}$	23.68	30.41
PF-350°C-1h	72.56 ± 1.15	$\textbf{8.86} \pm \textbf{0.29}$	18.58	33.84
PF-350°C-0.25 h	66.25 ± 0.27	6.75 ± 0.13	27.00	27.21
PF–350°C-0.5 h	$70.21 \pm \\ 0.90$	8.72 ± 0.20	21.07	32.41
PF-350°C-2h	$73.25 \pm \\2.12$	8.73 ± 0.57	18.02	33.99
PF-350°C-4h	$74.36 \pm \\ 0.85$	8.75 ± 0.11	16.89	34.60

^a Difference method was used to calculate the oxygen content.

2021). The literature claims that the increase in HTT temperature causes a higher C concentration in bio-crude, leading to a greater HHV and improved bio-crude's stability (Ross et al., 2010; Mahesh et al., 2021). The AHTT time has a meaningful effect on the C and H concentrations of crude oils. As shown in Table 6, when the AHTT time is raised from 0.25 to 4 h at 350 °C, the C concentration rises from 66.25 to 74.36 wt%, and the H concentration rises from 6.75 to 8.75 wt%. According to one research, as reaction time was raised, the C and H levels of the bio-crude raised, leading to a greater HHV in comparison to raw material (Mahesh et al., 2021).

The H/C atomic ratio of crude oils ranges from 1.30 to 1.48, while the O/C atomic ratio ranges from 0.17 to 0.37. Fig. 3 (3b) illustrated that utilizing PF instead of water at 350 $^{\circ}\text{C}$ for 1 h causes a drop in the O/C atomic ratio and a rise in the H/C atomic ratio. One research (R. Liu et al., 2018) observed the similar pattern for the O/C atomic ratio when two acids were added to municipal sludge during HTT; nevertheless, the H/C atomic ratio of crude oils dropped. H/C and O/C and atomic ratio fluctuation are significantly affected by AHTT temperature and time. As can be observed in Fig. 3 (3b), higher AHTT temperature and time are suitable to deoxygenate crude oils.

3.6. Boiling point distribution of AHTT's crude oils

The properties of the crude oils' devolatilization were evaluated using TGA analysis. Fig. 6 illustrates the TGA analysis data, which shows the crude oils' weight loss in different temperature ranges. Compounds having boiling temperatures lower than 40 °C are excluded from Fig. 6 since these compounds might be evaporated through DCM evaporation. The varying compositions of crude oils generated under various AHTT conditions resulted in a large disparity in their boiling point distributions. Generally, the fraction of crude oil that is most useful to generate liquid fuels is the fraction that is volatile below 400 °C (Seshasayee and Savage, 2020). The majority fraction of crude oil evaporates in the boiling range of lighter fuels include gasoline, kerosene, and diesel (57.58–83.09%).

Using PF instead of water increases the amount of lighter fuels from 72.30 to 80.57 wt%. The acidic nature of the process fluid plays a crucial role in this enhancement. Acids can effectively break more carboncarbon (C–C) bonds present in the PVC molecules (Wei et al., 2022). Essentially, the ability of the acid to facilitate the cleavage of C–C bonds allows for the generation of more light oil fractions (Seshasayee and Savage, 2020). One study (R. Liu et al., 2018) reported that HTT creates

 $[^]b$ HHV $\left(\!\frac{MJ}{Kg}\!\right)=0.3383$ C + $1.422 \!\left(H-\frac{O}{8}\right)$ (Average ultimate analysis results were used to calculate HHV).

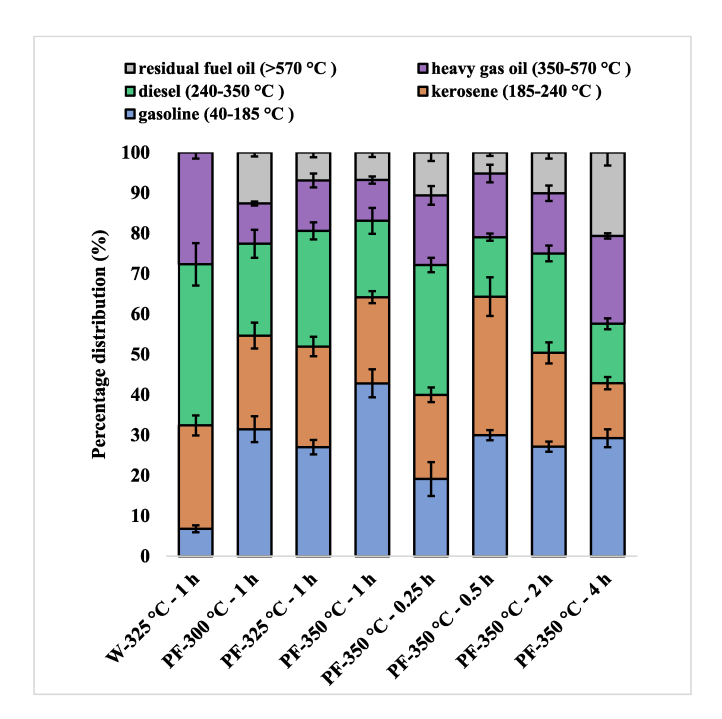


Fig. 6. Distribution of boiling points of the crude oils at various AHTT reaction conditions.

lighter oil fraction (gasoline, kerosene, and diesel) from bio-oil treated with HCl, HCOOH, HNO3, and, H2SO4. On the other hand, the fraction of residual fuel oil increases from 0 to 6.92 wt% using PF instead of water. The acidic environment might hinder the complete conversion of PVC into lighter fractions, leaving behind a greater proportion of unreacted or partially reacted material, which contributes to the residual fuel oil fraction. In addition, acid-catalyzed secondary reactions may occur, such as condensation reactions, leading to the formation of heavier compounds that contribute to the residual fuel oil fraction (Lu et al., 2020). As shown in Fig. 6, a higher AHTT temperature improves the quality of fuel oil since the amount of lighter oil fraction rises from 77.38 to 83.09 wt% and the amount of residual fuel oil decreases from 12.82 to 6.82 wt% with a temperature increase from 300 to 350 °C at 0.5 h. The reason could be the intensity of thermal cracking increases with increasing temperature (Seshasayee and Savage, 2020). One study reported that increasing the temperature during HTT of polypropylene from 400 to 450 °C considerably boosted the formation of lighter oil fraction (Seshasayee and Savage, 2020). Results indicate that AHTT time affects the fraction of lighter fuels. As seen in Fig. 6, the portion of lighter oil fraction increases from 72.14 to 83.09 wt% when AHTT time is raised from 0.25 to 1 h. However, when the AHTT time is increased from 1 to 4 h, the amount of lighter oil fraction decreased from 83.09 to 57.58 wt %, most likely owing to the synthesis of aromatic chemicals (Chen et al., 2019). Consequently, TGA results reveal that the boiling range of crude oil's components is similar to boiling range of refinery feedstocks. Therefore, it is possible that the crude oil can be refined utilizing the current systems of petroleum refining.

3.7. Chemical composition of AHTT's crude oils

GCMS was utilized to determine the chemical compositions of crude oils. Fig. 7 illustrates the percentage of the total identified area filled by different compounds of crude oils. Tables S3–S10 include the full GCMS data. During HTT, numerous cracking reactions happen following the system has produced sufficient energy for breaking the chemical link that binds polymers united (Bai et al., 2019). In accordance with the literature (López et al., 2011), most of the mass loss of PVC happens between 250 and 320 $^{\circ}$ C. At this stage, the primary reaction is

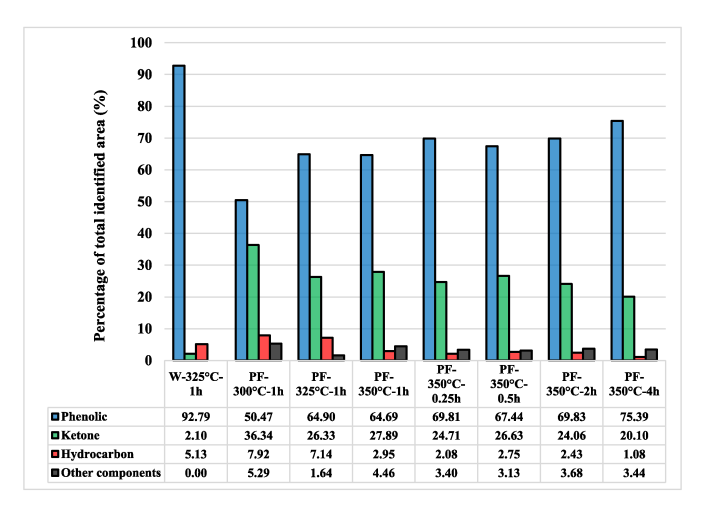


Fig. 7. Chemical composition of crude oils at different AHTT conditions.

dehydrochlorination, which produces volatile chemicals, which are mostly composed of HCl as well as extremely low amounts of light hydrocarbons such as toluene and benzene (Jordan et al., 2001).

According to the findings, crude oils produced from AHTT comprise mostly phenolic, ketone, and hydrocarbon components. Fig. 7 illustrates how using PF in place of water greatly reduces the proportion of phenolic and significantly enhances the proportion of ketone component. The proportion of phenolic components drops significantly from 92.79 to 64.90 wt%, the proportion of ketone components rises sharply from 2.10 to 26.33 wt%, and the proportion of hydrocarbons rises slightly from 5.13 to 7.14 wt%. Acid can enhance oxygenation reactions, facilitating the incorporation of oxygen atoms into organic molecules. This can result in an increase in oxygenated compounds like ketones within the crude oil composition (Ghalandari, 2023). One study showed that acid increases the proportion of oxygenated compounds like ketones detected in bio-oil (R. Liu et al., 2018; Chen et al., 2017).

The AHTT temperature significantly influences the production of ketone and phenolic components. The proportion of ketone components drops from 36.34 to 26.33 wt% as the temperature is raised from 300 to 325 °C, whereas the proportion of phenolic components rises from 50.47 to 64.90 wt%. The temperature sensitivity of different reaction pathways can lead to competition between pathways favoring the formation of ketone and phenolic components. At lower temperatures, pathways leading to ketone formation may dominate, while at higher temperatures, pathways favoring phenolic component formation become more prominente (Ghalandari et al., 2022). AHTT time has a substantial effect on the chemical composition of crude oil. As shown in Fig. 7, the phenolic components drop from 69.81 to 64.69 wt% as the AHTT time is raised from 0.25 to 1 h, but they increase to 75.39 wt% at 4 h. In addition, the proportion of ketone components rises from 24.71 to 27.89 wt% as the AHTT time is raised from 0.25 to 1 h but declines to 20.01 wt% as the AHTT time is extended to 4 h. When the AHTT time is increased from 0.25 to 4 h, the proportion of hydrocarbons drops from 2.08 to 1.08 wt%. Extended AHTT times allow more time for chemical equilibria to be established among various reaction intermediates. As a result, the relative proportions of phenolic, ketone, and hydrocarbon components may shift as the system reaches equilibrium. This can explain the observed increase in phenolic components and decrease in ketone components with longer AHTT times.

4. Conclusions

In this study, the possibility of using an HTC process fluid (PF) in hydrothermal treatment of waste polyvinyl chloride (WPVC) was investigated. The result showed that using PF and increasing reaction temperature from 300 to 350 $^{\circ}$ C enhanced the dechlorination efficiency

(DE) of WPVC. Increasing AHTT time from 0.25 to 1 h at 350 °C enhanced the DE of WPVC from 91.59 to 97.57%, but DE reduced slightly by extending AHTT time from 1 to 4 h. Moreover, using PF, increasing AHTT temperature and time enhanced the HHV of char and crude oils. Moreover, raising AHTT temperature significantly enhanced the DE of WPVC and improved the HHV of char and crude oil. The maximum HHV value of char and crude oil, which were obtained at 350 °C and 4 h, were 33.07 and 34.60 MJ/kg, respectively. In terms of combustion, AHTT char samples had higher T_i and lower T_f along with a moderate S index in comparison to WPVC. The ash of some char samples had a low IS, IF, IA, and medium Cl concentration. Most of the AHTT crude oil fraction evaporated within the boiling range of lighter fuels, comprising gasoline (19.12-42.83 wt%), kerosene (13.63-34.28 wt%), and diesel (14.71–32.16 wt%). The main components of AHTT crude oil (94.71-98.36 wt%) were phenolic, hydrocarbon, and ketone. In conclusion, AHTT significantly increases the chlorine elimination from WPVC and produces char and crude oil with high HHV and suitable combustion properties. The finding of this research might aid in the development of an effective thermochemical method for upcycling

The findings of this research hold promise for contributing to the development of an effective thermochemical method for upcycling WPVC, which could have significant economic implications. Further exploration of the scalability and feasibility of implementing the AHTT process on a larger scale is essential. Conducting pilot-scale studies to evaluate the practicality and economic viability of this thermochemical method for WPVC upcycling on an industrial level would be a valuable next step. Possible future research directions could include exploring potential applications for the char and crude oils produced through AHTT beyond their use as fuel sources could be another avenue for future research. Investigating their potential as feedstocks for chemical synthesis or other value-added products could provide further opportunities for waste minimization and resource recovery.

Funding

The material is based upon work partially supported by the National Science Foundation under Grant No. 2123495.

CRediT authorship contribution statement

Vahab Ghalandari: Conceptualization, Data curation, Formal analysis, Methodology, Writing – original draft, Writing – review & editing. **Toufiq Reza:** Conceptualization, Funding acquisition, Project administration, Writing – review & editing.

Declaration of competing interest

The authors declare that they have no known competing financial interests or personal relationships that could have appeared to influence the work reported in this paper.

Data availability

Data will be made available on request.

Acknowledgments

The authors acknowledge Adam Scannell from Florida Institute of Technology for assisting with the hydrothermal treatment experiments and sample characterization. The authors also acknowledge Andrew Wagner from Mainstream Engineering Corporation for assisting with GCMS.

Appendix A. Supplementary data

Supplementary data to this article can be found online at https://doi.org/10.1016/j.chemosphere.2024.142969.

References

- Abelouah, Mohamed Rida, Romdhani, Ilef, Ben-Haddad, Mohamed, Hajji, Sara, De-la-Torre, Gabriel E., Gaaied, Sonia, Barra, Issam, Mohamed, Banni, Aicha, Ait Alla, 2023. Binational survey using Mytilus galloprovincialis as a bioindicator of microplastic pollution: insights into chemical analysis and potential risk on humans. Sci. Total Environ. 870 (April), 161894 https://doi.org/10.1016/j.csitotany.2023.161804
- Bai, Bin, Jin, Hui, Fan, Chao, Cao, Changqing, Wei, Wenwen, Wen, Cao, 2019.
 Experimental investigation on liquefaction of plastic waste to oil in supercritical water. Waste Manag. 89 (April), 247–253. https://doi.org/10.1016/j.wasman.2019.04.017.
- Banivaheb, S., Ghalandari, V., Smith, H., Reza, M.T., 2022. SolvX: solvothermal conversion of mixed waste plastics in supercritical toluene in presence of Pd/C catalyst. J. Environ. Chem. Eng. 10 (6), 108622 https://doi.org/10.1016/j. iece.2022.108622.
- Bhat, Ajmal R., Najar, Mohd H., Dongre, Rajendra S., Akhter, Mohammad S., 2020. Microwave assisted synthesis of knoevenagel derivatives using water as green solvent. Current Research in Green and Sustainable Chemistry 3 (June), 100008. https://doi.org/10.1016/j.crgsc.2020.06.001.
- Bi, Hao, Wang, Zhiwei, Zhan, Hao, Leng, Lijian, Zeng, Zhiyong, Wang, Xinming, Liu, Huacai, Yin, Xiuli, Wu, Chuangzhi, 2022. Acid-promoted hydrothermal on Chinese herbal residue toward upgradation and denitrogenation capabilities. Fuel Process. Technol. 238 (December), 107518 https://doi.org/10.1016/j. fuproc.2022.107518.
- Chandrasekar, Ragavan, Kumar Rajendran, Harish, Vishnu, Priyan V., Selvaraju, Narayanasamy, 2022. Valorization of sawdust by mineral acid assisted hydrothermal carbonization for the adsorptive removal of bisphenol A: a greener approach. Chemosphere 303 (September), 135171. https://doi.org/10.1016/j. chemosphere.2022.135171.
- Chen, Wan Ting, Qian, Wanyi, Zhang, Yuanhui, Mazur, Zachary, Kuo, Chih-Ting, Scheppe, Karalyn, Schideman, Lance Charles, Sharma, Brajendra Kumar, 2017.
 Effect of ash on hydrothermal liquefaction of high-ash content algal biomass. Algal Res. 25 (July), 297–306. https://doi.org/10.1016/j.algal.2017.05.010.
- Chen, Wan-Ting, Jin, Kai, Wang, Nien-Hwa Linda, 2019. Use of supercritical water for the liquefaction of polypropylene into oil. ACS Sustain. Chem. Eng. 7 (4), 3749–3758. https://doi.org/10.1021/acssuschemeng.8b03841.
- Choi, Sun-A, Choi, Won-Il, Lee, Jin-Suk, Kim, Seung Wook, Lee, Gye-An, Yun, Jihyun, Park, Ji-Yeon, 2015. Hydrothermal acid treatment for sugar extraction from Golenkinia sp. Bioresour. Technol. 190 (August), 408–411. https://doi.org/10.1016/j.biortech.2015.04.121
- Čolnik, Maja, Kotnik, Petra, Knez, Željko, Škerget, Mojca, 2022. Degradation of polyvinyl chloride (PVC) waste with supercritical water. Processes 10 (10), 1940. https://doi. org/10.3390/pr10101940.
- De, Weerdt, Loïc, Sasao, Toshiaki, Compernolle, Tine, Van Passel, Steven, Jaeger, Simon De, 2020. The effect of waste incineration taxation on industrial plastic waste generation: a panel analysis. Resour. Conserv. Recycl. 157 (June), 104717 https://doi.org/10.1016/j.resconrec.2020.104717.
- Dong, Ning, Hui, Helong, Li, Songgeng, Lin, Du, 2023. Study on preparation of aromatic-rich oil by thermal dechlorination and fast pyrolysis of PVC. J. Anal. Appl. Pyrol. 169 (January), 105817 https://doi.org/10.1016/j.jaap.2022.105817.
- Du, Chuan, Li, Zhanping, 2023. Contamination and health risks of heavy metals in the soil of a historical landfill in Northern China. Chemosphere 313 (February), 137349. https://doi.org/10.1016/j.chemosphere.2022.137349.
- Duangchan, Kanyanat, Mohdee, Vanee, Punyain, Wikorn, Pancharoen, Ura, 2023.
 Mercury elimination from synthetic petroleum produced water using green solvent via liquid-liquid extraction: experimental, effective solubility behaviors and DFT investigation. J. Environ. Chem. Eng. 11 (2), 109296 https://doi.org/10.1016/j.ieee.2023.10296
- Endo, K., Emori, N., 2001. Dechlorination of poly (vinyl chloride) without anomalous units under high pressure and at high temperature in water. Polym. Degrad. Stabil. 74 (1), 113–117. https://doi.org/10.1016/S0141-3910(01)00108-2.
- Espro, C., Satira, A., Mauriello, F., Anajafi, Z., Moulaee, K., Iannazzo, D., Neri, G., 2021. Orange peels-derived hydrochar for chemical sensing applications. Sensor. Actuator. B Chem. 341 (August), 130016 https://doi.org/10.1016/j.snb.2021.130016.
- Gandon-Ros, Gerard, Soler, Aurora, Aracil, Ignacio, Francisca Gómez-Rico, María, 2020. Dechlorination of polyvinyl chloride electric wires by hydrothermal treatment using K2CO3 in subcritical water. Waste Manag. 102 (February), 204–211. https://doi. org/10.1016/j.wasman.2019.10.050.
- Geng, Xiaomeng, Song, Nan, Zhao, Youcai, Zhou, Tao, 2022. Waste plastic resource recovery from landfilled refuse: a novel waterless cleaning method and its costbenefit analysis. J. Environ. Manag. 306 (March), 114462 https://doi.org/10.1016/ j.jenvman.2022.114462.
- Ghalandari, V., 2023. Dechlorination of waste PVC (polyvinyl chloride) using hydrothermal liquefaction method. https://repository.fit.edu/etd/1328.
- Ghalandari, Vahab, Smith, Hunter, Volpe, Maurizio, Messineo, Antonio, Reza, Toufiq, 2022. Effect of acidic hydrochar on plastic crude oil produced from hydrothermal liquefaction of waste PVC. Processes 10 (12), 2538. https://doi.org/10.3390/pr10122538.

- Ghalandari, V., Volpe, M., Lùz, F.C., Messineo, A., Reza, T., 2023. Role of acidic hydrochar on dechlorination of waste PVC in high temperature hydrothermal treatment and fuel properties enhancement of solid residues. Waste Manag. 169, 125–136. https://doi.org/10.1016/j.wasman.2023.07.005.
- Ghalandari, V., Scannell, A., Reza, T., 2024. Elucidating dechlorination of waste polyvinyl chloride under high-temperature catalytic hydrothermal treatment. AIChE J. 70 (2), e18274 https://doi.org/10.1002/aic.18274.
- Hashimoto, K., Suga, S., Wakayama, Y., Funazukuri, T., 2008. Hydrothermal dechlorination of PVC in the presence of ammonia. J. Mater. Sci. 43, 2457–2462. https://doi.org/10.1007/s10853-007-2015-x.
- Hosseini, Beinabaj, Mahdi, Seyyed, Heydariyan, Hossein, Aleii, Hamed Mohammad, Ali, Hosseinzadeh, 2023. Concentration of heavy metals in leachate, soil, and plants in Tehran's landfill: investigation of the effect of landfill age on the intensity of pollution. Heliyon 9 (1), e13017. https://doi.org/10.1016/j.heliyon.2023.e13017.
- Islam, Md Tahmid, Sultana, Al Ibtida, Saha, Nepu, Klinger, Jordan L., Toufiq Reza, M., 2021. Pretreatment of biomass by selected type-III deep eutectic solvents and evaluation of the pretreatment effects on hydrothermal carbonization. Ind. Eng. Chem. Res. 60 (43), 15479–15491. https://doi.org/10.1021/acs.iecr.1c03068.
- Islam, Md Tahmid, Ibtida Sultana, Al, Chambers, Cadianne, Saha, Swarna, Saha, Nepu, Kirtania, Kawnish, Toufiq Reza, M., 2022. Recent progress on emerging applications of hydrochar. Energies 15 (24), 9340. https://doi.org/10.3390/en15249340.
- Jiang, Long-bo, Xing-zhong, Yuan, Li, Hui, Chen, Xiao-hong, Xiao, Zhi-hua, Liang, Jie, Leng, Li-jian, Guo, Zhi, Zeng, Guang-ming, 2016. Co-pelletization of sewage sludge and biomass: thermogravimetric analysis and ash deposits. Fuel Process. Technol. 145 (May), 109–115. https://doi.org/10.1016/j.fuproc.2016.01.027.
- Jordan, K.J., Suib, S.L., Koberstein, J.T., 2001. Determination of the degradation mechanism from the kinetic parameters of dehydrochlorinated poly(vinyl chloride) decomposition. J. Phys. Chem. B 105 (16), 3174–3181. https://doi.org/10.1021/ ip003223k.
- Kim, Sung Ho, Ahn, Seong-Yong, Kwak, Seung-Yeop, 2008. Suppression of dioxin emission in incineration of poly(vinyl chloride) (PVC) as hybridized with titanium dioxide (TiO2) nanoparticles. Appl. Catal. B Environ. 79 (3), 296–305. https://doi. org/10.1016/j.apcatb.2007.10.035.
- Li, Tian, Zhao, Peitao, Lei, Meng, Li, Zhaozhi, 2017. Understanding hydrothermal dechlorination of PVC by focusing on the operating conditions and hydrochar characteristics. Appl. Sci. 7 (3), 256. https://doi.org/10.3390/app7030256.
- Lin, Yousheng, Ma, Xiaoqian, Ning, Xingxing, Yu, Zhaosheng, 2015. TGA-FTIR analysis of Co-combustion characteristics of paper sludge and oil-palm solid wastes. Energy Convers. Manag. 89 (January), 727–734. https://doi.org/10.1016/j. enconman.2014.10.042.
- Lin, Yousheng, Ma, Xiaoqian, Peng, Xiaowei, Yu, Zhaosheng, Fang, Shiwen, Lin, Yan, Fan, Yunlong, 2016. Combustion, pyrolysis and char CO2-gasification characteristics of hydrothermal carbonization solid fuel from municipal solid wastes. Fuel 181 (October), 905–915. https://doi.org/10.1016/j.fuel.2016.05.031.
- Lin, Yousheng, Ge, Ya, Xiao, Hanmin, He, Qing, Wang, Wenhao, Chen, Baiman, 2020. Investigation of hydrothermal Co-carbonization of waste textile with waste wood, waste paper and waste food from typical municipal solid wastes. Energy 210 (November), 118606. https://doi.org/10.1016/j.energy.2020.118606.
- Ling, Mengxue, Ma, Dachao, Hu, Xuan, Liu, Zheng, Wang, Dongbo, Feng, Qingge, 2023. Hydrothermal treatment of polyvinyl chloride: reactors, dechlorination chemistry, application, and challenges. Chemosphere 316 (March), 137718. https://doi.org/10.1016/j.chemosphere.2022.137718.
- Liu, Renlong, Tian, Wenying, Kong, Shengyan, Meng, Yanghao, Wang, Huansheng, Zhang, Jinglai, 2018. Effects of inorganic and organic acid pretreatments on the hydrothermal liquefaction of municipal secondary sludge. Energy Convers. Manag. 174 (October), 661–667. https://doi.org/10.1016/j.enconman.2018.08.058.
- Liu, Yijie, Zhou, Chuanbin, Li, Feng, Liu, Hongju, Yang, Jianxin, 2020. Stocks and flows of polyvinyl chloride (PVC) in China: 1980-2050. Resour. Conserv. Recycl. 154 (March), 104584 https://doi.org/10.1016/j.resconrec.2019.104584.
- López, A., de Marco, I., Caballero, B.M., Laresgoiti, M.F., Adrados, A., 2011. Dechlorination of fuels in pyrolysis of PVC containing plastic wastes. Fuel Processing Technology, III International Congress on Energetic Engineering and Environment 92 (2), 253–260. https://doi.org/10.1016/j.fuproc.2010.05.008.
- Lu, Xiaoluan, Ma, Xiaoqian, Chen, Xinfei, Yao, Zhongliang, Zhang, Chaoyue, 2020. Co-hydrothermal carbonization of polyvinyl chloride and corncob for clean solid fuel production. Bioresour. Technol. 301 (April), 122763 https://doi.org/10.1016/j.biortech.2020.122763.
- Lu, Xinyu, Que, Han, Gu, Xiaoli, 2022. Facile fabrication of lignin containing cellulose films using water as green solvent. Eur. Polym. J. 168 (April), 111097 https://doi. org/10.1016/j.eurpolymj.2022.111097.
- Lv, Baoying, Zhao, Guohua, Li, Dongming, Liang, Chao, 2009. Dechlorination and oxidation for waste poly(vinylidene chloride) by hydrothermal catalytic oxidation on Pd/AC catalyst. Polym. Degrad. Stabil. 94 (7), 1047–1052. https://doi.org/ 10.1016/j.polymdegradstab.2009.04.004.
- Ma, S., Lu, J., Gao, J., 2002. Study of the low temperature pyrolysis of PVC. Energy Fuels 16 (2), 338–342. https://doi.org/10.1021/ef0101053.
- Ma, Dachao, Feng, Qingge, Chen, Boqing, Cheng, Xi, Chen, Kao, Jiao, Li, 2019. Insight into chlorine evolution during hydrothermal carbonization of medical waste model. J. Hazard Mater. 380 (December), 120847 https://doi.org/10.1016/j. ib.pares 2010.101677.
- Ma, Dachao, Liang, Liwu, Hu, Erfeng, Chen, Huaquan, Wang, Dongbo, He, Chao, Feng, Qingge, 2021. Dechlorination of polyvinyl chloride by hydrothermal treatment with cupric ion. Process Saf. Environ. Protect. 146 (February), 108–117. https://doi.org/10.1016/j.psep.2020.08.040.
- Mahesh, Danam, Ahmad, Shamshad, Kumar, Rajnish, Chakravarthy, S.R., Vinu, R., 2021. Hydrothermal liquefaction of municipal solid wastes for high quality bio-crude

- production using glycerol as Co-solvent. Bioresour. Technol. 339 (November), 125537 https://doi.org/10.1016/j.biortech.2021.125537.
- Meng, Tian-Tian, Zhang, Hua, Fan, Lü, Shao, Li-Ming, He, Pin-Jing, 2021. Comparing the effects of different metal oxides on low temperature decomposition of PVC. J. Anal. Appl. Pyrol. 159 (October), 105312 https://doi.org/10.1016/j.jaap.2021.105312.
- Ning, Xiaojun, Teng, Haipeng, Wang, Guangwei, Zhang, Jianliang, Zhang, Nan, Huang, Chunchao, Wang, Chuan, 2020. Physiochemical, structural and combustion properties of hydrochar obtained by hydrothermal carbonization of waste polyvinyl chloride. Fuel 270 (June), 117526. https://doi.org/10.1016/j.fuel.2020.117526.
- Nyberg, Björn, Harris, Peter T., Kane, Ian, Maes, Thomas, 2023. Leaving a plastic legacy: current and future scenarios for mismanaged plastic waste in rivers. Sci. Total Environ. 869 (April), 161821 https://doi.org/10.1016/j.scitotenv.2023.161821.
- Peng, Yujie, Wang, Yunpu, Ke, Linyao, Dai, Leilei, Wu, Qiuhao, Cobb, Kirk, Yuan, Zeng, Zou, Rongge, Liu, Yuhuan, Ruan, Roger, 2022. A review on catalytic pyrolysis of plastic wastes to high-value products. Energy Convers. Manag. 254 (February), 115243 https://doi.org/10.1016/j.enconman.2022.115243.
- Pettersson, R. Patrik, Olsson, Marie, 1998. A nitric acid-hydrogen peroxide digestion method for trace element analysis of milligram amounts of plankton and periphyton by total-reflection X-ray fluorescence spectrometry. J. Anal. Atomic Spectrom. 13 (7), 609–613. https://doi.org/10.1039/A708575C.
- Poerschmann, J., Weiner, B., Woszidlo, S., Koehler, R., Kopinke, F.-D., 2015a. Hydrothermal carbonization of poly(vinyl chloride). Chemosphere 119 (January), 682–689. https://doi.org/10.1016/j.chemosphere.2014.07.058.
- Poerschmann, J., Weiner, B., Woszidlo, S., Koehler, R., Kopinke, F.-D., 2015b. Hydrothermal carbonization of poly(vinyl chloride). Chemosphere 119 (January), 682–689. https://doi.org/10.1016/j.chemosphere.2014.07.058.
- Quaid, T., Ghalandari, V., Reza, T., 2022. Effect of synthesis process, synthesis temperature, and reaction time on chemical, morphological, and quantum properties of carbon dots derived from loblolly pine. Biomass 2 (4), 250–263. https://doi.org/ 10.3390/biomass2040017.
- Rahimi, AliReza, García, Jeannette M., 2017. Chemical recycling of waste plastics for new materials production. Nat. Rev. Chem 1 (6), 1–11. https://doi.org/10.1038/ s41570-017-0046
- Ignatyev, I.A., 2014. Recycling of polymers: a review. ChemSusChem. Wiley Online Library. https://chemistry-europe.onlinelibrary.wiley.com/doi/10.1002/cssc. 201300898. (Accessed 17 February 2023).
- Reza, M. Toufiq, Lynam, Joan G., Helal Uddin, M., Coronella, Charles J., 2013a. Hydrothermal carbonization: fate of inorganics. Biomass Bioenergy 49 (February), 86–94. https://doi.org/10.1016/j.biombioe.2012.12.004.
- Reza, M. Toufiq, Lynam, Joan G., Helal Uddin, M., Coronella, Charles J., 2013b. Hydrothermal carbonization: fate of inorganics. Biomass Bioenergy 49 (February), 86–94. https://doi.org/10.1016/j.biombioe.2012.12.004.
- Ross, A.B., Biller, P., Kubacki, M.L., Li, H., Lea-Langton, A., Jones, J.M., 2010. Hydrothermal processing of microalgae using alkali and organic acids. Fuel 89 (9), 2234–2243. https://doi.org/10.1016/j.fuel.2010.01.025.
- Sarrion, Andres, de la Rubia, Angeles, Charles, Coronella, Mohedano, Angel F., Diaz, Elena, 2022. Acid-mediated hydrothermal treatment of sewage sludge for nutrient recovery. Sci. Total Environ. 838 (September), 156494 https://doi.org/ 10.1016/j.scitoteny.2022.156494.
- Seshasayee, Mahadevan Subramanya, Savage, Phillip E., 2020. Oil from plastic via hydrothermal liquefaction: production and characterization. Appl. Energy 278 (November), 115673. https://doi.org/10.1016/j.apenergy.2020.115673.
- Shen, Yafei, 2016. Dechlorination of poly(vinyl chloride) wastes via hydrothermal carbonization with lignin for clean solid fuel production. Ind. Eng. Chem. Res. 55 (44), 11638–11644. https://doi.org/10.1021/acs.iecr.6b03365.
- Shen, Yafei, 2020. A review on hydrothermal carbonization of biomass and plastic wastes to energy products. Biomass Bioenergy 134 (March), 105479. https://doi.org/ 10.1016/j.biombioe.2020.105479
- Shen, Maocai, Tong, Hu, Huang, Wei, Song, Biao, Qin, Meng, Yi, Huan, Zeng, Guangming, Zhang, Yaxin, 2021. Can incineration completely eliminate plastic wastes? An investigation of microplastics and heavy metals in the bottom ash and fly ash from an incineration plant. Sci. Total Environ. 779 (July), 146528 https://doi.org/10.1016/j.scitotenv.2021.146528.
- Shen, Maocai, Xiong, Weiping, Song, Biao, Zhou, Chengyun, Almatrafi, Eydhah, Zeng, Guangming, Zhang, Yaxin, 2022. Microplastics in landfill and leachate: occurrence, environmental behavior and removal strategies. Chemosphere 305 (October), 135325. https://doi.org/10.1016/j.chemosphere.2022.135325.
- Shin, S.M., Yoshioka, T., Okuwaki, A., 1998. Dehydrochlorination behavior of flexible PVC pellets in NaOH solutions at elevated temperature. J. Appl. Polym. Sci. 67 (13), 2171–2177. https://doi.org/10.1002/(SICI)1097-4628(19980328)67:13<2171:: AID-APP7>3.0.CO;2-B.
- Shinohara, Naohide, Uchino, Kanako, 2020. Diethylhexyl phthalate (DEHP) emission to indoor air and transfer to house dust from a PVC sheet. Sci. Total Environ. 711 (April), 134573 https://doi.org/10.1016/j.scitotenv.2019.134573.
- Takeshita, Yukitoshi, Kato, Kiyoshi, Takahashi, Kazue, Sato, Yoshiyuki, Nishi, Shiro, 2004. Basic study on treatment of waste polyvinyl chloride plastics by hydrothermal decomposition in subcritical and supercritical regions. J. Supercrit. Fluids 31 (2), 185–193. https://doi.org/10.1016/j.supflu.2003.10.006.
- Tejaswini, M.S.S.R., Pathak, Pankaj, Ramkrishna, Seeram, Sankar Ganesh, P., 2022. A comprehensive review on integrative approach for sustainable management of plastic waste and its associated externalities. Sci. Total Environ. 825 (June), 153973 https://doi.org/10.1016/j.scitotenv.2022.153973.
- Torres, D., Jiang, Y., Sanchez-Monsalve, D.A., Leeke, G.A., 2020. Hydrochloric acid removal from the thermogravimetric pyrolysis of PVC. J. Anal. Appl. Pyrol. 149 (August), 104831 https://doi.org/10.1016/j.jaap.2020.104831.

- Tortosa Masiá, A.A., Buhre, B.J.P., Gupta, R.P., Wall, T.F., 2007. Characterising ash of biomass and waste. Fuel Processing Technology, Impacts of Fuel Quality on Power Production 88 (11), 1071–1081. https://doi.org/10.1016/j.fuproc.2007.06.011.
- Wang, Qi, Zhang, Jianliang, Wang, Guangwei, Wang, Haiyang, Sun, Minmin, 2018. Thermal and kinetic analysis of coal with different waste plastics (PVC) in cocombustion. Energy Fuels 32 (2), 2145–2155. https://doi.org/10.1021/acs.energyfuels.7b03268.
- Wei, Yingyuan, Fakudze, Sandile, Zhang, Yiming, Ma, Ru, Shang, Qianqian, Chen, Jianqiang, Liu, Chengguo, Chu, Qiulu, 2022. Co-hydrothermal carbonization of pomelo peel and PVC for production of hydrochar pellets with enhanced fuel properties and dechlorination. Energy 239 (January), 122350. https://doi.org/ 10.1016/j.energy.2021.122350.
- Xiu, F.R., Wang, Y., Yu, X., Li, Y., Lu, Y., Zhou, K., He, J., Song, Z., Gao, X., 2020. A novel safety treatment strategy of DEHP-rich flexible polyvinyl chloride waste through low-temperature critical aqueous ammonia treatment. Sci. Total Environ. 708, 134532 https://doi.org/10.1016/j.scitotenv.2019.134532.
- Xu, Zhuo, Kolapkar, Shreyas S., Zinchik, Stas, Bar-Ziv, Ezra, McDonald, Armando G., 2020. Comprehensive kinetic study of thermal degradation of polyvinylchloride (PVC). Polym. Degrad. Stabil. 176 (June), 109148 https://doi.org/10.1016/j. polymdegradstab.2020.109148.
- Xu, Xianbao, Zhu, Daan, Jian, Qiwei, Wang, Xiaonuan, Zheng, Xiaohu, Xue, Gang, Liu, Yanbiao, Xiang, Li, Hassan, Gamal Kamel, 2023. Treatment of industrial ferric sludge through a facile acid-assisted hydrothermal reaction: focusing on dry mass reduction and hydrochar recyclability performance. Sci. Total Environ. 869 (April), 161879 https://doi.org/10.1016/j.scitotenv.2023.161879.
- Yang, Wenchao, Li, Xianguo, Liu, Shishi, Feng, Lijuan, 2014. Direct hydrothermal liquefaction of undried macroalgae Enteromorpha prolifera using acid catalysts. Energy Convers. Manag. 87 (November), 938–945. https://doi.org/10.1016/j. enconman.2014.08.004.
- Yang, Maolin, Zhao, Peitao, Cui, Xin, Geng, Fan, Guo, Qingjie, 2021. Kinetics study on hydrothermal dechlorination of poly(vinyl chloride) by in-situ sampling. Environ. Technol. Innov. 23 (August), 101703 https://doi.org/10.1016/j.eti.2021.101703.

- Yao, Zhongliang, Ma, Xiaoqian, 2018. Characteristics of Co-hydrothermal carbonization on polyvinyl chloride wastes with bamboo. Bioresour. Technol. 247 (January), 302–309. https://doi.org/10.1016/j.biortech.2017.09.098.
- Yoshioka, Toshiaki, Kameda, Tomohito, Imai, Shogo, Noritsune, Masahiko, Okuwaki, Akitsugu, 2008. Dechlorination of poly(vinylidene chloride) in NaOH/ethylene glycol as a function of NaOH concentration, temperature, and solvent. Polym. Degrad. Stabil. 93 (10), 1979–1984. https://doi.org/10.1016/j.polymdegradstab.2008.06.008.
- Zhang, Yifan, Yuan, Ying, Tan, Wenbing, 2022. Influences of humic acid on the release of polybrominated diphenyl ethers from plastic waste in landfills under different environmental conditions. Ecotoxicol. Environ. Saf. 230 (January), 113122 https://doi.org/10.1016/j.ecoenv.2021.113122.
- Zhang, Jing, Zhang, Lin, Lin, Chuanjin, Wang, Cuiping, Zhao, Peitao, Li, Yimin, 2023. Co-hydrothermal carbonization of polyvinyl chloride and lignocellulose biomasses: influence of biomass feedstock on fuel properties and combustion behaviors. Sci. Total Environ. 868 (April), 161532 https://doi.org/10.1016/j.scitoteny.2023.161532
- Zhao, Di, Zhang, Jianliang, Wang, Guangwei, Conejo, Alberto N., Xu, Runsheng, Wang, Haiyang, Zhong, Jianbo, 2016. Structure characteristics and combustibility of carbonaceous materials from blast furnace flue dust. Appl. Therm. Eng. 108 (September), 1168–1177. https://doi.org/10.1016/j.applthermaleng.2016.08.020.
- Zhao, Peitao, Li, Zhaozhi, Li, Tian, Yan, Weijie, Ge, Shifu, 2017. The study of nickel effect on the hydrothermal dechlorination of PVC. J. Clean. Prod. 152 (May), 38–46. https://doi.org/10.1016/j.jclepro.2017.03.101.
- Zhao, Yanling, Jia, Guangchao, Shang, Yili, Zhao, Peitao, Cui, Xin, Guo, Qingjie, 2022. Chlorine migration during hydrothermal carbonization of recycled paper wastes and fuel performance of hydrochar. Process Saf. Environ. Protect. 158 (February), 495–502. https://doi.org/10.1016/j.psep.2021.12.041.
- Zou, Shuping, Wu, Yulong, Yang, Mingde, Li, Chun, Tong, Junmao, 2009. Thermochemical catalytic liquefaction of the marine microalgae Dunaliella tertiolecta and characterization of bio-oils. Energy Fuels 23 (7), 3753–3758. https://doi.org/10.1021/ef9000105.